Amide-Stabilized, Diamagnetic Chromium(II) Nitrosyl Complexes[1]

Eric W. Jandciu, Jane Kuzelka, Peter Legzdins,* Steven J. Rettig,[†] and
Kevin M. Smith

*Department of Chemistry, The University of British Columbia,
Vancouver, British Columbia, Canada V6T 1Z1*

Received November 30, 1998

Treatment of $Cr(NO)(N^iPr_2)_3$ with 2 equiv of $PhCO_2H$ affords $Cr(NO)(N^iPr_2)(O_2CPh)_2$ (**1**) in good yields. Reaction of CpNa·DME with **1** produces $CpCr(NO)(N^iPr_2)(OC(O)Ph)$ (**2**), which subsequently yields a series of 18-valence-electron (18e) complexes, $CpCr(NO)(N^iPr_2)(R)$ (R = η^1-Cp (**3**), CH_2SiMe_3 (**4**), η^1-CH_2Ph (**5**), Ph (**6**), CPh=CH_2 (**7**), C≡CCMe₃ (**8**), C≡CPh (**9**)) when treated with additional CpNa·DME or 1 equiv of the appropriate $R_2Mg·x$(dioxane) reagent. **2**−**9** are low-spin ($S = 0$) compounds, and their electronic stability is attributed to the strong, synergic π-bonding interactions present in the $[Cr(NO)(N^iPr_2)]^{2+}$ core, as indicated both by the NMR and IR spectra of these complexes and by the solid-state molecular structures of **2**−**4**. The "strong-field" nitrosyl and amide ligands also enforce a diamagnetic configuration on the 14e bis(hydrocarbyl) complexes $Cr(NO)(N^iPr_2)R_2$ (R = CH_2SiMe_3 (**10**), CH_2Ph (**11**), *o*-tolyl (**12**)), which are obtained in good yields by reaction of **1** with 2 equiv of the corresponding $R_2Mg·x$(dioxane) reactants. The solid-state molecular structures of **10** and **11** have also been established by single-crystal X-ray crystallographic analyses. Variable-temperature NMR spectroscopy was employed to study the fluxional processes occurring in **1**, **10**, and **11**.

Introduction

In synthetic organometallic chemistry even the most reasonable and appealing target molecules remain inaccessible in the absence of suitable synthetic precursors. A particular case in point involves diamagnetic, unsaturated, mid-valent hydrocarbyl compounds of chromium, which are potentially useful complexes for studying the chemistry of Cr−C σ bonds. Interestingly, examples of such species are readily available for the heavier group 6 congeners molybdenum and tungsten. For example, a plethora of Cp′M(NO)R₂ compounds (Cp′ = Cp, Cp*; M = Mo, W; R = hydrocarbyl ligand) can be obtained by treatment of their dichloro precursors with organomagnesium reagents.[2] Unfortunately, the corresponding Cp′Cr(NO)Cl₂ precursor compounds are not known, and attempts to prepare them via oxidation of Cr(I) or Cr(0) nitrosyl complexes result in the dissociation of the NO ligand.[3]

Our recent investigations into ligand-bonding properties and electronic configurations of CpCr(NO)-containing species suggested that π-donor ligands might stabilize organometallic Cr(II) nitrosyl complexes.[4] After our attempts to synthesize such compounds from more

reduced CpCr(NO)-containing species were unsuccessful, we next turned our attention to an inorganic precursor that *already possesses* a π-donor-stabilized Cr(II) nitrosyl entity, namely $Cr(NO)(N^iPr_2)_3$.[5] This approach proved to be successful, and so we now describe in this paper the first well-characterized Cr(II) nitrosyl hydrocarbyl compounds, which have been synthesized via amine-elimination and salt-metathesis reactions of the tris(amide) complex. Portions of this work have been previously communicated.[6]

Experimental Section

General Methods. All reactions and subsequent manipulations were performed under anhydrous and anaerobic conditions by employing conventional Schlenk, vacuum-line, and inert-atmosphere glovebox techniques unless otherwise specified. General procedures routinely employed in these laboratories have been described in detail previously.[7] Glassware was first heated in an oven at 200 °C to remove any moisture and then cooled to room temperature under vacuum prior to use. Solvents were purchased from either Aldrich or BDH Chemicals and were purified under a continuous flow of dinitrogen by employing published procedures.[8] Et_2O and hexanes were predried over CaH_2 and then distilled from Na/benzophenone;

† Deceased October 27, 1998.
(1) π-Bonding and Reactivity in Transition Metal Nitrosyl Complexes, 6. Part 5: Reference 4.
(2) (a) Legzdins, P.; Veltheer, J. E. *Acc. Chem. Res.* **1993**, *26*, 41. (b) Veltheer, J. E.; Legzdins, P. In *Synthetic Methods of Organometallic and Inorganic Chemistry*; Herrmann, W. A., Ed.; Thieme: Stuttgart, Germany, 1997; Vol. 8; pp 79−85.
(3) Legzdins, P.; McNeil, W. S.; Rettig, S. J.; Smith, K. M. *J. Am. Chem. Soc.* **1997**, *119*, 3513.
(4) Legzdins, P.; McNeil, W. S.; Smith, K. M.; Poli, R. *Organometallics* **1998**, *17*, 615.

(5) (a) Bradley, D. C.; Newing, C. W. *J. Chem. Soc., Chem. Commun.* **1970**, 219. (b) Bradley, D. C.; Newing, C. W.; Chisholm, M. H.; Kelly, R. L.; Haitko, D. A.; Little, D.; Cotton, F. A.; Fanwick, P. E. *Inorg. Chem.* **1980**, *19*, 3010. (c) Odom, A. L.; Cummins, C. C.; Protasiewicz, J. D. *J. Am. Chem. Soc.* **1995**, *117*, 6613.
(6) Kuzelka, J.; Legzdins, P.; Rettig, S. J.; Smith, K. M. *Organometallics* **1997**, *16*, 3569.
(7) Legzdins, P.; Rettig, S. J.; Ross, K. J.; Batchelor, R. J.; Einstein, F. W. B. *Organometallics* **1995**, *14*, 5579.
(8) Perrin, D. D.; Armarego, W. L. F.; Perrin, D. R. *Purification of Laboratory Chemicals*, 3rd ed.; Wiley-Interscience: New York, 1986.

pentane was distilled from Na/benzophenone; CH_2Cl_2 was distilled from CaH_2; THF was predried over CaH_2 and then distilled from K metal. All solvents were deaerated with argon or dinitrogen for 10–15 min prior to use or were vacuum-transferred from the appropriate drying agent.

Nitric oxide was obtained from Linde Union Carbide Specialty Gas, and prior to use, higher oxides of nitrogen were removed from it by passage of the gas through a column of activated silica gel at −78 °C. Benzoic acid was purchased from Fisher and was purified by sublimation prior to use. Anhydrous $CrCl_3$ was also obtained from Fisher and was used as received. Dicyclopentadiene was purchased from Aldrich and was thermally cracked to produce C_5H_6. HCl was purchased from Aldrich as a 1.0 M Et_2O solution and was diluted with additional Et_2O to a concentration of 0.01 M prior to use. Hexamethyldisiloxane was purchased from Aldrich and was distilled from sodium metal prior to use. *t*-BuNC was purchased from Aldrich and dried over 4 Å sieves. CpNa·DME[9] and $R_2Mg·x$(dioxane) ($x \approx 1$)[10] were prepared according to literature procedures. $Cr(NO)(N^iPr_2)_3$ was prepared by the reaction of $CrCl_3(THF)_3$ with lithium diisopropylamide, and the subsequent nitrosylation was effected with approximately 1.5 equiv of NO gas.[5] All spectral and characterization data for the new complexes isolated during this work were obtained in the manner previously specified.[7]

Preparation of $Cr(NO)(N^iPr_2)(O_2CPh)_2$ (1). A solution of red $Cr(NO)(N^iPr_2)_3$ (1.74 g, 4.55 mmol) in a minimum amount of Et_2O (150 mL) was prepared in a Schlenk tube. In a second Schlenk tube benzoic acid (1.11 g, 9.09 mmol) was dissolved in Et_2O (25 mL). The benzoic acid solution was then slowly cannulated into the stirred $Cr(NO)(N^iPr_2)_3$ solution. Shortly after completion of the addition of the benzoic acid solution, the reaction mixture changed from red to orange, and an orange precipitate was deposited. After being stirred for approximately 1 h, during which time no further color change was evident, the supernatant solution was removed from the mixture via cannula. The solid remaining in the flask was washed with Et_2O (2 × 30 mL), and the washings were added to the supernatant solution and placed in a freezer at −30 °C overnight to obtain additional precipitate. The collected orange solid, $Cr(NO)(N^iPr_2)(O_2CPh)_2$ (1), was dried under vacuum at ambient temperatures for 1 h.

Preparation of $CpCr(NO)(N^iPr_2)(O_2CPh)$ (2). A 50 mL Erlenmeyer flask was charged with $Cr(NO)(N^iPr_2)(O_2CPh)_2$ (1; 0.334 g, 0.79 mmol). The orange powder was dissolved in THF (10 mL) to obtain a red solution, which was then frozen solid at −196 °C in a cold well. Crystalline CpNa·DME (0.140 g, 0.79 mmol) was added to the frozen solution, and the mixture was then warmed to room temperature while being stirred. Once the frozen solution had melted, an almost immediate color change from red to dark green occurred. After being stirred for 2 h, the mixture was filtered through Celite (1 × 1 cm) supported on a medium-porosity glass frit. The THF solvent was removed from the filtrate under vacuum, and the residue was then redissolved in Et_2O and cooled overnight at −30 °C to induce the deposition of dark green crystals of $CpCr(NO)(N^iPr_2)(O_2CPh)$ (2), which were collected by filtration, washed with hexanes, and dried under vacuum at ambient temperatures.

Preparation of $CpCr(NO)(N^iPr_2)(\eta^1$-Cp) (3). A 25 mL Erlenmeyer flask was charged with $CpCr(NO)(N^iPr_2)(O_2CPh)$ (2; 0.050 g, 0.14 mmol) and crystalline CpNa·DME (0.024 g, 0.14 mmol) and was cooled to −196 °C in a cold well. THF (15 mL) was slowly run down the walls of the vial in a dropwise fashion, thereby allowing the THF to freeze upon contact with the cold solids. The vial was then warmed to room temperature

while its contents were being stirred. The initially green mixture gradually became red over a 1 h period at room temperature. The THF was removed from the final mixture in vacuo, the remaining solid was dissolved in Et_2O, and the solution was filtered through Celite (0.5 × 2 cm) supported on glass wool in a glass pipet. The volume of the filtrate was diminished under reduced pressure, and an equal volume of hexanes was then added. The volume of this new solution was again reduced under vacuum, and it was then placed in a freezer at −30 °C overnight to induce the deposition of dark red crystals of **3**, which were collected by filtration.

Alternative Preparation of $CpCr(NO)(N^iPr_2)(\eta^1$-Cp) (3). A Schlenk tube was charged with $Cr(NO)(N^iPr_2)(O_2CPh)_2$ (**2**; 0.200 g, 0.47 mmol) and CpLi (0.068 g, 0.94 mmol). THF (30 mL) was vacuum-transferred onto the two solids, and the frozen solution was then warmed slowly to room temperature while being stirred. The initially pale orange solution gradually became dark red over a 1 h period. The solvent was removed from the final mixture in vacuo, and the residue was dissolved in Et_2O and filtered through Celite (1 × 1 cm) supported on a medium-porosity glass frit. The same procedure for crystallization as described in the preceding paragraph was employed to obtain analytically pure, dark red crystals of **3**.

Preparation of $CpCr(NO)(N^iPr_2)(CH_2SiMe_3)$ (4). A 25 mL Erlenmeyer flask was charged with $CpCr(NO)(N^iPr_2)(O_2CPh)$ (**2**; 0.096 g, 0.26 mmol) and $(CH_2SiMe_3)_2Mg·x$(dioxane) ($x \approx 1$; 0.041 g, 0.26 mmol) and was cooled to −196 °C in a cold well. THF (15 mL), previously cooled to −30 °C, was slowly run down the walls of the flask in a dropwise fashion, thereby allowing the THF to freeze on contact with the cold solids. The flask was then placed on a rotary evaporator and slowly rotated in order to melt the frozen THF. Upon melting, the initially green mixture gradually became red over a 30 min period as it was warmed to room temperature. Stirring was continued for another 1 h, after which time the THF was removed under vacuum. The remaining solid was dissolved in pentane and filtered through Celite (1 × 1 cm) supported on a medium-porosity glass frit. The volume of the red filtrate was reduced under vacuum before being placed in a freezer at −30 °C to induce crystallization. Red crystals of analytically pure $CpCr(NO)(N^iPr_2)(CH_2SiMe_3)$ (4) were collected by filtration after 24 h at −30 °C.

Treatment of $CpCr(NO)(N^iPr_2)(CH_2SiMe_3)$ (4) with Dilute HCl. A solution of $CpCr(NO)(N^iPr_2)(CH_2SiMe_3)$ (0.010 g, 0.030 mmol) was prepared in Et_2O (10 mL). To this was added a dilute solution of HCl in Et_2O (3 mL, 0.01 M) via cannula, whereupon an immediate color change from red to dark red-brown occurred. Stirring of the mixture for 15 min resulted in the deposition of a small amount of blue-green precipitate on the walls of the reaction Schlenk. Solution IR spectroscopy identified no new nitrosyl-containing products, and further stirring overnight resulted in no visible or spectroscopic changes. Subsequent addition of excess dilute HCl afforded additional blue-green precipitate, which was isolated and identified as $[CpCrCl_2]_2$ by mass spectrometry.[11]

Preparation of $CpCr(NO)(N^iPr_2)(\eta^1$-$CH_2Ph)$ (5), $CpCr(NO)(N^iPr_2)(Ph)$ (6), $CpCr(NO)(N^iPr_2)(CPh=CH_2)$ (7), $CpCr(NO)(N^iPr_2)(C≡CCMe_3)$ (8), and $CpCr(NO)(N^iPr_2)(C≡CPh)$ (9). These five complexes were synthesized in a manner identical with that described for compound **4** by employing $(PhCH_2)_2Mg·x$(dioxane), $Ph_2Mg·x$(dioxane), $(CH_2=CPh)_2Mg·x$(dioxane), $Me_3CC≡CLi$, and $(PhC≡C)_2Li$, respectively, in place of $(CH_2SiMe_3)_2Mg·x$(dioxane). Like **4**, complexes **5**, **6**, and **8** were isolated by crystallization from pentane at −30 °C, whereas analytically pure complexes **7** and **9** were obtained by crystallization from Et_2O at the same temperature.

Preparation of $Cr(NO)(N^iPr_2)(CH_2SiMe_3)_2$ (10). THF (25 mL) was vacuum-transferred onto bis(benzoate) **1** (0.500 g,

(9) Smart, J. C.; Curtis, C. J. *Inorg. Chem.* **1977**, *16*, 1788.

(10) (a) Andersen, R. A.; Wilkinson, G. *J. Chem. Soc., Dalton Trans.* **1977**, 809. (b) Dryden, N. H.; Legzdins, P.; Trotter, J.; Yee, V. C. *Organometallics* **1991**, *10*, 2857.

(11) Kohler, F. H.; de Cao, R.; Ackermann, K.; Sedlmair, J. Z. *Z. Naturforsch., B* **1983**, *38*, 1406.

1.17 mmol) and $(Me_3SiCH_2)_2Mg \cdot x$(dioxane) ($x \approx 1$; 0.363 g, 2.34 mmol). The mixture changed from an orange suspension to a clear, red solution as it was warmed slowly to room temperature over 30 min. After being stirred for an additional 1 h at ambient temperatures, the solvent was then removed from the final mixture under vacuum, and the red residue was extracted with hexanes (5×10 mL). The extracts were filtered through Celite (2×5 cm) supported on a medium-porosity glass frit. The solvent was removed from the filtrate under vacuum to obtain a red powder. Dark red needles of **10** were obtained by recrystallization of this material from $(Me_3Si)_2O$.

Preparation of $Cr(NO)(N^iPr_2)(CH_2Ph)_2$ (11) and Cr-$(NO)(N^iPr_2)(o\text{-tolyl})_2$ (12). These two complexes were synthesized in a manner identical with that described in the preceding paragraph by employing $(CH_2Ph)_2Mg \cdot x$(dioxane) and $(o\text{-tolyl})_2Mg \cdot x$(dioxane), respectively, in place of $(Me_3SiCH_2)_2$-$Mg \cdot x$(dioxane) and with the entire reaction mixture being kept at or below 0 °C at all times during the procedure. Also, Et_2O was used as the solvent in order to facilitate its removal. Both complexes **11** and **12** were isolated by crystallization from hexanes.

Preparation of $Cr(NO)(N^iPr_2)(CH_2SiMe_3)(C(=N^tBu)\text{-}CH_2SiMe_3)$ (13). A solution of $Cr(NO)(N^iPr_2)(CH_2SiMe_3)_2$ (0.150 g, 0.42 mmol) was prepared in Et_2O (10 mL) and cooled to -196 °C in a cold well. ^tBuNC (48 μL, 0.42 mmol) was diluted in Et_2O (3 mL) and cooled to -30 °C in a freezer. The former solution was allowed to melt and stirred as the cooled ^tBuNC solution was added in a dropwise manner. A nearly immediate color change from deep red to pale orange occurred. The reaction mixture was stirred for an additional 10 min before the solvent was removed in vacuo. The remaining solid was dissolved in hexamethyldisiloxane, and the solution was filtered through Celite (0.5×2 cm) supported on glass wool in a glass pipet. The volume of the filtrate was reduced, and it was then placed in a freezer at -30 °C to induce the formation of orange, microcrystalline **13**.

X-ray Crystallographic Analyses of Complexes 2−4, 10, and 11. Crystallographic data are collected in Table 1. The final unit cell parameters were based on 25 reflections with $2\theta = 16.3-25.4°$ for **2**, 22 161 reflections with $2\theta = 4.0-60.1°$ for **3**, 7654 reflections with $2\theta = 4.0-63.6°$ for **4**, 17 441 reflections with $2\theta = 4.0-61.3°$ for **10**, and 5847 reflections with $2\theta = 4.0-61.1°$ for **11**. The data were processed[12] and corrected for Lorentz and polarization effects and for absorption (empirical, based on azimuthal scans for 2 and on three-dimensional analyses of symmetry-equivalent data using fourth-order spherical harmonics for **3**, **4**, **10**, and **11**). A linear decay correction was applied for **2**.

The structures of **2−4** were solved by the Patterson method and those of **10** and **11** by direct methods. The analyses of **2**, **4**, **10**, and **11** were initiated in the centrosymmetric space group $P\bar{1}$ on the basis of the E statistics, these choices being confirmed by subsequent calculations. The asymmetric units of **4**, **10**, and **11** contain two independent molecules. All non-hydrogen atoms were refined with anisotropic thermal parameters. Hydrogen atoms were fixed in calculated positions with C−H = 0.98 Å and $B_H = 1.2B_{bonded\ atom}$ for **2**, **4**, **10**, and **11** and were refined with isotropic thermal parameters for **3**.

The hydrogen atoms of interest in **11** (i.e. H(1,2,15)) were also refined isotropically. Secondary extinction corrections were not necessary. Neutral-atom scattering factors and anomalous dispersion corrections were taken from ref 13. Selected bond lengths and angles for the five compounds appear in Tables 2−6. Atomic coordinates, anisotropic thermal parameters, all bond lengths and angles, torsion angles, intermolecular contacts, and least-squares planes are provided as Supporting Information.

Results and Discussion

Analytical data and a numbering scheme for all new complexes isolated during this work are presented in Table 7, and their mass spectroscopic and IR spectral data are collected in Table 8. ^1H and $^{13}C\{^1H\}$ NMR spectroscopic data for complexes **1−13** are given in Table 9.

Amine-Elimination Reactions. The organometallic chromium(II) nitrosyl compounds described in this paper are all derived from $Cr(NO)(N^iPr_2)_3$ via selective substitution of two of the amide ligands. Similar amine-elimination reactions have been developed for the synthesis of olefin-polymerization-catalyst precursors from tetrakis(amido)titanium, -zirconium, and -hafnium complexes. For example, protonolysis of two amide ligands from group 4 $M(NR_2)_4$ species with the protonated form of the appropriate incoming ligand provides *ansa*-metallocene,[14,15] amide-functionalized cyclopentadienyl,[16−20] or chelating diamide[21−23] compounds. In addition, recent work by Cummins and co-workers has demonstrated that highly selective amine-elimination reactions are possible. By using MeI, alcohols, and amine hydrohalides as "deprotecting" agents, they have crafted elaborate ligand sets from Ti(IV) mixed-tetrakis-(amide)[24] and Cr(VI) tris(amide) nitride[25] precursors. The resulting halides or alkoxides can then be alkylated to form high-valent, d^0 organometallic species. We have successfully employed a similar protocol with our system for the selective replacement of two amide ligands by carboxylate groups, as shown in eq 1. This transformation is specific for the $Cr(NO)(N^iPr_2)_3$ reactant shown; the analogous $Cr(NO)(N(SiMe_3)_2)_3$ simply does not react

(12) (a) teXsan, Crystal Structure Analysis Package, Version 1.8; Molecular Structure Corp., The Woodlands, TX, 1997. (b) d*TREK, Area Detector Software; Molecular Structure Corp., The Woodlands, TX, 1997.

(13) (a) *International Tables for X-ray Crystallography*; Kynoch Press: Birmingham, U.K. (present distributor Kluwer Academic: Boston, MA), 1974; Vol. IV, pp 99−102. (b) *International Tables for Crystallography*; Kluwer Academic: Boston, MA, 1992; Vol. C, pp 200−206.

(14) (a) Diamond, G. M.; Jordan, R. F.; Petersen, J. L. *Organometallics* **1996**, *15*, 4030. (b) Christopher, J. N.; Diamond, G. M.; Jordan, R. F.; Petersen, J. L. *Organometallics* **1996**, *15*, 4038. (c) Diamond, G. M.; Jordan, R. F.; Petersen, J. L. *Organometallics* **1996**, *15*, 4045. (d) Diamond, G. M.; Jordan, R. F.; Petersen, J. L. *J. Am. Chem. Soc.* **1996**, *118*, 8024.

(15) Herzog, T. A.; Zubris, D. L.; Bercaw, J. E. *J. Am. Chem. Soc.* **1996**, *118*, 11988.

(16) (a) Hughes, A. K.; Meetsma, A.; Teuben, J. H. *Organometallics* **1993**, *15*, 1936. (b) Hughes, A. K.; Marsh, S. M. B.; Howard, J. A. K.; Ford, P. S. *J. Organomet. Chem.* **1997**, *528*, 195.

(17) (a) Herrmann, W. A.; Morawietz, M. J. A.; Priermeir, T. *Angew. Chem., Int. Ed. Engl.* **1994**, *33*, 1946. (b) Herrmann, W. A.; Morawietz, M. J. A. *J. Organomet. Chem.* **1994**, *482*, 169.

(18) Mu, Y.; Piers, W. E.; MacGillivray, L. R.; Zaworotko, M. J. *Polyhedron* **1995**, *14*, 1.

(19) Carpenetti, D. W.; Kloppenburg, L.; Kupec, J. T.; Petersen, J. L. *Organometallics* **1996**, *15*, 1572.

(20) McKnight, A. L.; Masood, M. A.; Waymouth, R. M.; Strauss, D. A. *Organometallics* **1997**, *16*, 2879.

(21) (a) Guérin, F.; McConville, D. H.; Vittal, J. J. *Organometallics* **1996**, *15*, 5586. (b) Scollard, J. D.; McConville, D. H.; Vittal, J. J. *Organometallics* **1997**, *16*, 4415.

(22) (a) Baumann, R.; Davis, W. M.; Schrock, R. R. *J. Am. Chem. Soc.* **1997**, *119*, 3830. (b) Aizenberg, M.; Turculet, L.; Davis, W. M.; Schattenmann, F.; Schrock, R. R. *Organometallics* **1998**, *17*, 4795. (c) Baumann, R.; Schrock, R. R. *J. Organomet. Chem.* **1998**, *557*, 69.

(23) Gibson, V. C.; Kimberley, B. S.; White, A. J. P.; Williams, D. J.; Howard, P. *Chem. Commun.* **1998**, 313.

(24) (a) Johnson, A. R.; Wanandi, P. W.; Cummins, C. C.; Davis, W. M. *Organometallics* **1994**, *13*, 2907. (b) Johnson, A. R.; Davis, W. M.; Cummins, C. C. *Organometallics* **1996**, *15*, 3825.

(25) (a) Odom, A. L.; Cummins, C. C. *Organometallics* **1996**, *15*, 898. (b) Odom, A. L.; Cummins, C. C. *Polyhedron* **1998**, *17*, 675.

Table 1. Crystallographic Data for Complexes 2−4, 10, and 11

	2[a]	**3**[b]	**4**[b]	**10**[b]	**11**[b]
formula	$C_{18}H_{24}CrN_2O_3$	$C_{16}H_{24}CrN_2O$	$C_{15}H_{30}CrN_2OSi$	$C_{14}H_{36}CrN_2OSi_2$	$C_{20}H_{28}CrN_2O$
fw	368.40	312.37	334.50	356.62	364.45
color, habit	brown, plate	red, prism	red, irregular	red, plate	red, prism
cryst size, mm	$0.05 \times 0.25 \times 0.35$	$0.10 \times 0.25 \times 0.35$	$0.25 \times 0.30 \times 0.45$	$0.20 \times 0.45 \times 0.60$	$0.45 \times 0.30 \times 0.20$
cryst system	triclinic	orthorhombic	triclinic	triclinic	triclinic
space group	$P\bar{1}$ (No. 2)	*Pbca* (No. 61)	$P\bar{1}$ (No. 2)	$P\bar{1}$ (No. 2)	$P\bar{1}$ (No. 2)
a, Å	9.6028(7)	10.093(2)	10.568(2)	11.2004(12)	7.4431(10)
b, Å	11.292(1)	14.5436(3)	13.584(3)	12.8210(9)	8.682(2)
c, Å	8.954(1)	21.8340(9)	14.158(3)	16.979(2)	15.453(3)
α, deg	95.786(10)	90	89.945(6)	91.035(7)	95.805(4)
β, deg	96.597(8)	90	85.289(3)	91.743(3)	98.073(3)
γ, deg	105.207(7)	90	71.2344(12)	113.6640(8)	95.757(3)
V, Å^3	922.0(2)	3205.0(4)	1917.3(6)	2231.0(3)	977.0(3)
Z	2	8	4	4	2
T, °C	21(1)	−93(1)	−93(1)	−93(1)	−93(1)
ρ_{calcd}, g cm^{-3}	1.327	1.295	1. 159	1.062	1.239
$F(000)$	388	1328	720	776	388
μ(Mo Kα), cm^{-1}	6.20	7.12	6.58	6.20	5.94
transmissn factors	0.88−1.00	0.85−1.00[c]	0.85−1.00[c]	0.63−1.00[c]	0.84−1.00[c]
scan type	ω−2θ	0.5° oscilln	0.5° oscilln	0.5° oscilln	0.5° oscilln
scan range, deg	1.10 + 0.35 tan θ				
scan speed, deg min^{-1}	16 (up to 9 scans)				
no. of data images		460 (70 s)	460 (35 s)	460 (60 s)	462 (10 s)
ϕ oscilln range (χ − 90), deg		0.0−190.0	0.0−190.0	0.0−190.0	0.0−190.0
ω oscilln range (χ − 90), deg		−22.0 to +18.0	−22.0 to +18.0	−22.0 to +18.0	−23.0 to +18.0
$2\theta_{max}$, deg	55.0	60.1	60.0	60.0	61.1
data collected	h, $\pm k$, $\pm l$	full sphere	full sphere	full sphere	full sphere
crystal decay, %	1.73				
total no. of rflns	4488	30 062	17 805 ($2\theta_{max} = 63.8°$)	20 644	8979
no. of unique rflns	4233	4396	8354 ($2\theta_{max} = 60°$)	8207	4457
R_{merge}	0.026	0.067	0.056	0.040	0.047
no. of rflns with I G $3\sigma(I)$	2289	2450	3839	4520	2480
no. of variables	217	277	361	361	229
$R(F)$ ($I \geq 3\sigma(I)$)	0.035	0.035	0.042	0.056	0.042
R_w	0.032	0.066	0.073	0.100	0.039
GOF	1.68	1.68	1.88	2.25	1.23
max Δ/σ (last cycle)	0.002	0.002	0.0003	0.0007	0.0009
residual density, e Å^{-3}	−0.23, +0.18	−0.74, +0.70	−0.74, +0.73	−0.61, +0.54	−0.69, +0.63

[a] Conditions and definitions: Rigaku AFC6S diffractometer, Mo Kα radiation (λ = 0.710 69 Å), graphite monochromator, takeoff angle 6.0°, aperture 6.0 $\times$ 6.0 mm at a distance of 285 mm from the crystal, stationary background counts at each end of the scan (scan/background time ratio 2:1), $\sigma^2(F^2) = [S^2(C + 4B)]/Lp^2$ (S = scan rate, C = scan count, B = normalized background count), function minimized $\sum w(|F_o| - |F_c|)^2$, where $w = 4F_o^2/\sigma^2(F_o^2)$, $R = \sum||F_o| - |F_c||/\sum|F_o|$, $R_w = (\sum w(|F_o| - |F_c|)^2/\sum w|F_o|^2)^{1/2}$, and GOF = $[\sum w(|F_o| - |F_c|)^2/(m - n)]^{1/2}$. Values given for R, R_w, and GOF are based on those reflections with $I \geq 3\sigma(I)$. [b] Conditions and definitions: Rigaku AFC7/ADSC Quantum 1 CCD diffractometer, Mo Kα radiation (λ = 0.710 69 Å), graphite monochromator, takeoff angle 6.0°, aperture 94 $\times$ 94 mm at a distance of 39.2 mm from the crystal, oscillation width 0.5°, $\sigma^2(F^2) = 3[(C + B)^{1/2}/Lp]$ (C = scan count, B = background count), function minimized $\sum w(|F_o^2 - F_c^2|)^2$ where $w = 1/\sigma^2(F_o^2)$, $R = \sum||F_o| - |F_c||/\sum|F_o|$, $R_w = (\sum w(|F_o^2 - F_c^2|)^2/\sum w|F_o^2|^2)^{1/2}$, and GOF = $[\sum w(|F_o^2| - |F_c^2|)^2/(m - n)]^{1/2}$. Values for R_w and GOF are based on all unique data. [c] Single-step correction for absorption, decay, and scaling based on symmetry analysis of redundant data.

under identical experimental conditions.
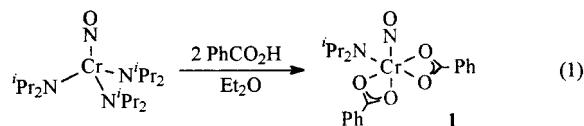
Nevertheless, favorable solubility properties and relative rates of amine elimination combine to make conversion 1 a particularly convenient route to the Cr(II) nitrosyl mono(amide) precursor required for the subsequent preparation of alkyl complexes. Thus, treatment of a red, Et$_2$O solution of Cr(NO)(N^{i}Pr$_2$)$_3$ with 2 equiv of PhCO$_2$H leads to an orange solution that readily

deposits the less soluble Cr(NO)(N^{i}Pr$_2$)(O$_2$CPh)$_2$ (**1**). If less than 2 equiv of benzoic acid is used, the final reaction mixture contains the bis(benzoate) **1** and unreacted Cr(NO)(N^{i}Pr$_2$)$_3$ (^{1}H NMR, C$_6$D$_6$). Reaction with a third equivalent of benzoic acid appears to occur at a slower rate. IR spectroscopic monitoring of the reaction of bis(benzoate) **1** with PhCO$_2$H in CH$_2$Cl$_2$ reveals that the ν(NO) band due to **1** gradually diminishes in intensity and that the final green solution is devoid of IR bands in the nitrosyl-stretching region. Related protonolysis reactions have previously been reported for Cr(NO)(N^{i}Pr$_2$)$_3$ and Cr(N)(N^{i}Pr$_2$)$_3$ with alcohols.[5,25]

In the absence of an X-ray crystallographic analysis, the molecular structure of **1** must be deduced from its

Table 2. Selected Bond Lengths (Å) and Bond Angles (deg) for Complex 2[a]

Cr(1)−O(2)	1.975(2)	Cr(1)−N(1)	1.670(2)
Cr(1)−N(2)	1.840(2)	Cr(1)−C(1)	2.272(3)
Cr(1)−C(2)	2.233(3)	Cr(1)−C(3)	2.185(3)
Cr(1)−C(4)	2.249(3)	Cr(1)−C(5)	2.292(3)
Cr(1)−CP	1.95	O(1)−N(1)	1.194(3)
O(2)−C(6)	1.295(3)	O(3)−C(6)	1.220(3)
N(2)−C(13)	1.485(3)	N(2)−C(14)	1.484(3)
C(1)−C(2)	1.388(4)	C(1)−C(5)	1.415(4)
C(2)−C(3)	1.397(4)	C(3)−C(4)	1.396(4)
C(4)−C(5)	1.383(4)	C(6)−C(7)	1.502(4)
O(2)−Cr(1)−N(1)	94.19(10)	O(2)−Cr(1)−N(2)	101.95(8)
O(2)−Cr(1)−CP	116.3	N(1)−Cr(1)−N(2)	99.5(1)
N(1)−Cr(1)−CP	116.6	N(2)−Cr(1)−CP	123.2
Cr(1)−O(2)−C(6)	124.7(2)	Cr(1)−N(1)−O(1)	165.7(2)
Cr(1)−N(2)−C(13)	126.7(2)	Cr(1)−N(2)−C(14)	121.0(2)
C(13)−N(2)−C(14)	112.3(2)	C(2)−C(1)−C(5)	108.5(3)
C(1)−C(2)−C(3)	107.7(3)	C(2)−C(3)−C(4)	108.0(3)
C(3)−C(4)−C(5)	108.9(3)	C(1)−C(5)−C(4)	107.0(3)
O(2)−C(6)−O(3)	125.5(3)	O(2)−C(6)−C(7)	114.4(3)
N(1)−Cr(1)−N(2)−C(13)		−0.9(2)	

[a] CP refers to the unweighted centroid of the C(1−5) ring.

Table 3. Selected Bond Lengths (Å) and Bond Angles (deg) for Complex 3[a]

Cr(1)−N(1)	1.660(2)	Cr(1)−N(2)	1.845(2)
Cr(1)−C(1)	2.245(2)	Cr(1)−C(2)	2.215(2)
Cr(1)−C(3)	2.276(2)	Cr(1)−C(4)	2.295(2)
Cr(1)−C(5)	2.264(2)	Cr(1)−C(6)	2.195(2)
Cr(1)−CP	1.918	O(1)−N(1)	1.213(2)
N(2)−C(11)	1.488(2)	N(2)−C(12)	1.485(2)
C(1)−C(2)	1.411(3)	C(1)−C(5)	1.394(3)
C(2)−C(3)	1.414(3)	C(3)−C(4)	1.385(3)
C(4)−C(5)	1.412(3)	C(6)−C(7)	1.461(3)
C(6)−C(10)	1.453(3)	C(7)−C(8)	1.349(3)
C(8)−C(9)	1.447(3)	C(9)−C(10)	1.354(3)
N(1)−Cr(1)−N(2)	99.87(7)	N(1)−Cr(1)−C(6)	91.66(7)
N(1)−Cr(1)−CP	120.5	N(2)−Cr(1)−C(6)	99.24(7)
N(2)−Cr(1)−CP	124.1	C(6)−Cr(1)−CP	115.2
Cr(1)−N(1)−O(1)	170.1(1)	Cr(1)−N(2)−C(11)	120.8(1)
Cr(1)−N(2)−C(12)	127.2(1)	C(11)−N(2)−C(12)	112.0(1)
C(2)−C(1)−C(5)	107.4(2)	C(1)−C(2)−C(3)	107.9(2)
C(2)−C(3)−C(4)	108.1(2)	C(3)−C(4)−C(5)	107.9(2)
C(1)−C(5)−C(4)	108.6(2)	Cr(1)−C(6)−C(7)	112.1(1)
Cr(1)−C(6)−C(10)	110.5(1)	C(7)−C(6)−C(10)	104.1(2)
C(6)−C(7)−C(8)	109.5(2)	C(7)−C(8)−C(9)	108.5(2)
C(8)−C(9)−C(10)	108.2(2)	C(6)−C(10)−C(9)	109.7(2)
N(1)−Cr(1)−N(2)−C(11)		−175.9(1)	

[a] CP refers to the unweighted centroid of the C(1−5) ring.

spectroscopic properties (Tables 8 and 9). Its ν(NO) band at 1710 cm^{-1} (Nujol) is higher in energy than the value of 1641 cm^{-1} reported for the tris(amide) precursor,[5] indicative of a decrease in electron density at Cr. Other, weaker IR bands observed at 1599, 1518, 1493, and 1420 cm^{-1} are attributable to the benzoate ligands. However, the modes of attachment (η^1 or η^2) of the benzoate ligands to the metal center cannot be unambiguously

(26) When the difference between the IR bands for the symmetric and asymmetric stretches of a carboxylate complex is greater than the difference observed in the free carboxylate, it is indicative of η^1 coordination, while a lower difference suggests η^2 coordination. In the case of compound **2** this difference is clearly greater and is in agreement with the molecular structure showing the benzoate ligand coordinated in an η^1 fashion. Compound **1** is not as clearly defined, since two benzoate ligands are present, although when the difference between the highest and lowest carboxylate bands is used, the value still lies below that of the free benzoate difference and thus implies η^2 coordination. Nakamoto, K. *Infrared and Raman Spectra of Inorganic and Coordination Compounds*, 5th ed.; Wiley: New York, 1997; Part B, pp 59−60. See also: Cotton, F. A.; Wilkinson, G. *Advanced Inorganic Chemistry*, 5th ed.; Wiley-Interscience: New York, 1988; pp 483−484.

Table 4. Selected Bond Lengths (Å) and Bond Angles (deg) for Complex 4[a]

Cr(1)−N(1)	1.653(2)	Cr(2)−N(3)	1.657(2)
Cr(1)−N(2)	1.832(2)	Cr(2)−N(4)	1.834(2)
Cr(1)−C(1)	2.238(3)	Cr(2)−C(16)	2.216(3)
Cr(1)−C(2)	2.207(3)	Cr(2)−C(17)	2.273(3)
Cr(1)−C(3)	2.275(2)	Cr(2)−C(18)	2.305(3)
Cr(1)−C(4)	2.294(3)	Cr(2)−C(19)	2.281(3)
Cr(1)−C(5)	2.276(3)	Cr(2)−C(20)	2.245(3)
Cr(1)−C(6)	2.111(2)	Cr(2)−C(21)	2.103(2)
Cr(1)−CP(1)	1.92	Cr(2)−CP(2)	1.93
O(1)−N(1)	1.211(2)	O(2)−N(3)	1.204(2)
N(2)−C(10)	1.486(3)	N(4)−C(25)	1.473(4)
N(2)−C(13)	1.489(3)	N(4)−C(28)	1.493(3)
C(1)−C(2)	1.396(4)	C(16)−C(17)	1.404(4)
C(1)−C(5)	1.398(4)	C(16)−C(20)	1.392(4)
C(2)−C(3)	1.397(4)	C(17)−C(18)	1.387(4)
C(3)−C(4)	1.380(4)	C(18)−C(19)	1.383(4)
C(4)−C(5)	1.413(4)	C(19)−C(20)	1.397(4)
N(1)−Cr(1)−N(2)	100.12(10)	N(3)−Cr(2)−N(4)	99.42(11)
N(1)−Cr(1)−C(6)	97.45(10)	N(3)−Cr(2)−C(21)	95.67(10)
N(1)−Cr(1)−CP(1)	119.4	N(3)−Cr(2)−CP(2)	120.5
N(2)−Cr(1)−C(6)	98.61(10)	N(4)−Cr(2)−C(21)	99.79(10)
N(2)−Cr(1)−CP(1)	124.2	N(4)−Cr(2)−CP(2)	124.3
C(6)−Cr(1)−CP(1)	112.1	C(21)−Cr(2)−CP(2)	111.8
Cr(1)−N(1)−O(1)	168.0(2)	Cr(2)−N(3)−O(2)	169.6(2)
Cr(1)−N(2)−C(10)	127.2(2)	Cr(2)−N(4)−C(25)	127.2(2)
Cr(1)−N(2)−C(13)	120.7(2)	Cr(2)−N(4)−C(28)	120.2(2)
C(10)−N(2)−C(13)	112.1(2)	C(25)−N(4)−C(28)	112.6(2)
C(2)−C(1)−C(5)	108.5(3)	C(17)−C(16)−C(20)	107.3(3)
C(1)−C(2)−C(3)	107.8(3)	C(16)−C(17)−C(18)	108.8(3)
C(2)−C(3)−C(4)	108.2(3)	C(17)−C(18)−C(19)	107.2(3)
C(3)−C(4)−C(5)	108.6(3)	C(18)−C(19)−C(20)	109.2(3)
C(1)−C(5)−C(4)	106.8(3)	C(16)−C(20)−C(19)	107.5(3)
Cr(1)−C(6)−Si(1)	122.87(13)	Cr(2)−C(21)−Si(2)	121.27(12)
N(1)−Cr(1)−N(2)−C(10)		−0.6(2)	

[a] CP(1,2) refer to the unweighted centroids of the C(1−5, 16−20) rings, respectively.

Table 5. Selected Bond Lengths (Å) and Bond Angles (deg) for Complex 10

Cr(1)−N(1)	1.616(2)	Cr(2)−N(3)	1.637(3)
Cr(1)−N(2)	1.763(2)	Cr(2)−N(4)	1.770(2)
Cr(1)−C(1)	2.026(3)	Cr(2)−C(15)	1.992(3)
Cr(1)−C(2)	1.986(3)	Cr(2)−C(16)	2.022(3)
O(1)−N(1)	1.221(3)	O(2)−N(3)	1.207(3)
N(2)−C(9)	1.464(4)	N(4)−C(23)	1.461(4)
N(2)−C(12)	1.491(3)	N(4)−C(26)	1.477(4)
N(1)−Cr(1)−N(2)	102.91(12)	N(3)−Cr(2)−N(4)	102.60(11)
N(1)−Cr(1)−C(1)	102.85(12)	N(3)−Cr(2)−C(15)	102.47(14)
N(1)−Cr(1)−C(2)	103.46(12)	N(3)−Cr(2)−C(16)	103.73(13)
N(2)−Cr(1)−C(1)	113.72(11)	N(4)−Cr(2)−C(15)	116.33(12)
N(2)−Cr(1)−C(2)	115.68(11)	N(4)−Cr(2)−C(16)	112.57(13)
C(1)−Cr(1)−C(2)	115.72(12)	C(15)−Cr(2)−C(16)	116.52(13)
Cr(1)−N(1)−O(1)	179.0(3)	Cr(2)−N(3)−O(2)	179.5(2)
Cr(1)−N(2)−C(9)	138.4(2)	Cr(2)−N(4)−C(23)	136.8(2)
Cr(1)−N(2)−C(12)	103.2(2)	Cr(2)−N(4)−C(26)	103.8(2)
C(9)−N(2)−C(12)	118.3(2)	C(23)−N(4)−C(26)	119.1(2)
Cr(1)−C(1)−Si(1)	117.39(14)	Cr(2)−C(15)−Si(3)	128.8(2)
Cr(1)−C(2)−Si(2)	130.6(2)	Cr(2)−C(16)−Si(4)	120.2(2)
N(1)−Cr(1)−N(2)−C(9)		−1.2(3)	

assigned on the basis of these bands due to their intermediate values and the possibility that one or more of them may well correspond to aromatic C−C bond stretches.[26]

Variable-temperature ^{1}H NMR spectroscopy proved to be very useful in delineating the fluxional processes present in **1**. At −30 °C, the spectrum in toluene-d_8 displays four sharp doublets for the amide methyl groups, two multiplets for the methine moieties, and two distinct resonances for the *ortho* protons of the O_2CPh

Table 6. Selected Bond Lengths (Å) and Bond Angles (deg) for Complex 11

Cr(1)−N(1)	1.629(2)	Cr(1)−N(2)	1.772(2)
Cr(1)−C(1)	2.063(3)	Cr(1)−C(2)	2.352(3)
Cr(1)−C(8)	2.085(3)	O(1)−N(1)	1.219(2)
N(2)−C(15)	1.484(3)	N(2)−C(18)	1.464(3)
C(1)−C(2)	1.450(4)	C(2)−C(3)	1.412(4)
C(2)−C(7)	1.417(3)	C(3)−C(4)	1.374(4)
C(8)−C(9)	1.493(3)	C(9)−C(10)	1.384(3)

N(1)−Cr(1)−N(2)	102.63(9)	N(1)−Cr(1)−C(1)	99.37(12)
N(1)−Cr(1)−C(2)	103.93(10)	N(1)−Cr(1)−C(8)	99.80(10)
N(2)−Cr(1)−C(1)	109.42(11)	N(2)−Cr(1)−C(2)	140.61(13)
N(2)−Cr(1)−C(8)	108.28(10)	C(1)−Cr(1)−C(2)	37.62(10)
Cr(1)−N(1)−O(1)	178.1(2)	Cr(1)−N(2)−C(15)	105.32(15)
Cr(1)−N(2)−C(18)	137.36(15)	C(15)−N(2)−C(18)	117.2(2)
Cr(1)−C(1)−C(2)	82.1(2)	Cr(1)−C(2)−C(1)	60.31(14)
Cr(1)−C(8)−C(9)	114.80(15)	C(8)−C(9)−C(10)	121.8(2)
N(2)−C(15)−C(16)	111.7(2)	N(2)−C(15)−C(17)	111.7(2)
C(16)−C(15)−C(17)	112.1(2)	N(2)−C(18)−C(19)	110.3(2)

N(1)−Cr(1)−N(2)−C(18)		−0.8(3)	

ligands. These are features of a compound possessing C_1 symmetry. At ambient temperatures two broad singlets are observed for the amide Me groups, along with two additional broad singlets for the amide CH groups, and only a single sharp resonance corresponding to the ipso carbons of the benzoate groups. A species approaching C_s symmetry results upon warming to 76 °C, as indicated by the methyl signals collapsing to a single broad resonance, the methine signals shifting toward each other, and the single ipso carbon resonance sharpening further.

To explain these observations, it is necessary to invoke two different fluxional processes. The first is amide rotation about the Cr−N bond, as indicated by the variation of the amide resonances with temperature. The second is a geometric shift at the metal center converting enantiomers **A** and **B,** as depicted in eq 2.

(2)
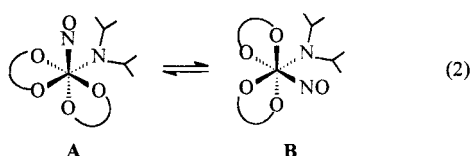
At low temperature both of these processes are slow, resulting in four different methyl environments and two different benzoate groups. Because the complex is chiral, the amide ligand methyl groups are diastereotopic and thus each has a unique chemical shift. At room temperature the geometric shift has quickened such that only two methyl environments exist in the molecule, since any influence from the benzoate ligands will have become an averaged effect from both ligands. At high temperature, when amide rotation is also occurring rapidly, only one methyl group environment is present and gives rise to the observed singlet.

While these data are consistent with several of the possible geometric isomers of Cr(NO)(N^{i}Pr$_2$)(O$_2$CPh)$_2$, a pseudo-octahedral arrangement with bidentate carboxylates and the amide and nitrosyl ligands occupying mutually cis positions is a reasonable candidate for the low-temperature limiting structure of **1**.

Introduction of a Cp Ligand. Treatment of **1** with 1 equiv of CpNa·DME affords CpCr(NO)(N^{i}Pr$_2$)(OC(O)-

Ph) (**2**), as illustrated in eq 3. The presence of a ν(CO)

(3)
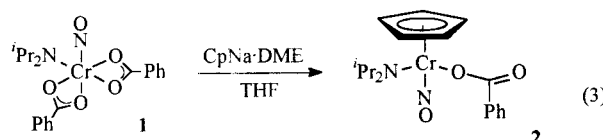
band at 1629 cm^{-1} in the Nujol-mull IR spectrum of **2** suggests that the remaining benzoate ligand adopts an η^1-coordination mode.[26] The room-temperature ^{1}H NMR spectrum of **2** displays distinct doublets for each of the four amide methyl groups, thereby indicating that any rotation about the Cr−N linkage is slow on the NMR time scale. Consistently, the solid-state molecular structure of **2** (Figure 1 and Table 2) provides evidence for the presence of a strong Cr−amide π-bonding interaction. Specifically, the Cr−N bond is short,[27] and the Cr−NC$_2$ unit is planar. Significantly, the amide plane is aligned with the Cr−nitrosyl bond, a conformation that permits π-donation from the filled amide nitrogen p orbital into the empty Cr d orbital that lies in the plane perpendicular to the Cr−NO axis.[28] This electronically preferred conformation is observed even though it places one of the amide ^{i}Pr groups close to the Cp ligand. These distinctive structural features are also evident in the solid-state molecular structures of the two other CpCr-(NO)(N^{i}Pr$_2$)X complexes we have characterized crystallographically (vide infra).

Our previous analysis of π-bonding in cyclopentadienylchromium complexes indicated that the presence of the Cr−N π-bond increases the HOMO−LUMO gap of CpCr(NO)(NR$_2$)X complexes, which in turn improves the relative stability of the low-spin, diamagnetic electronic configuration.[3] On the other hand, CpCr(NO)Cl$_2$, which lacks this significant π-bonding interaction, is calculated to have a triplet ground state;[4] the consequent weakening of the Cr−NO bond renders this compound unstable with respect to loss of the nitrosyl ligand.[3] Finally, it may be noted that reactions analogous to that shown in eq 3 using Cp* or HB(pyrazolyl)$_3$ salts instead of CpNa·DME in our hands afforded no tractable products. One possible rationale for the difference is that, with these larger ligands, the preferred Cr−amide conformation cannot be achieved due to increased intramolecular steric repulsion, thereby leading to the disruption of the Cr−N π-bond and subsequent decomposition via NO dissociation.

Electronically Saturated Hydrocarbyl Complexes. The reaction of **2** with a second equivalent of

(27) Cr−N bond lengths range from 1.77 to 2.12 Å for nonbridging Cr(II) amides; see: (a) Bradley, D. C.; Hursthouse, M. B.; Newing, C. W.; Welch, A. J. *J. Chem. Soc., Chem. Commun.* **1972**, 567. (b) Sim, G. A.; Woodhouse, D. I.; Knox, G. R. *J. Chem. Soc., Dalton Trans.* **1979**, 83. (c) Edema, J. J. H.; Gambarotta, S.; Meetsma, A.; Spek, A. L.; Smeets, W. J. J.; Chiang, M. Y. *J. Chem. Soc., Dalton Trans.* **1993**, 789. (d) Fryzuk, M. D.; Leznoff, D. B.; Rettig, S. R. *Organometallics* **1995**, *14*, 5193.
(28) (a) Ashby, M. T.; Enemark, J. H. *J. Am. Chem. Soc.* **1986**, *108*, 730. (b) Hubbard, J. L.; McVicar, W. K. *Inorg. Chem.* **1992**, *31*, 910. (c) Legzdins, P.; Ross, K. J.; Sayers, S. F.; Rettig, S. J. *Organometallics* **1997**, *16*, 190.
(29) (a) Piper, T. S.; Wilkinson, G. *J. Inorg. Nucl. Chem.* **1956**, *3*, 104. (b) Cotton, F. A.; Musco, A.; Yagupsky, G. *J. Am. Chem. Soc.* **1967**, *89*, 6136. (c) Cotton, F. A.; Legzdins, P. *J. Am. Chem. Soc.* **1968**, *90*, 6232. (d) Calderon, J. L.; Cotton, F. A.; Legzdins, P. *J. Am. Chem. Soc.* **1969**, *91*, 2528. (e) Hames, B. W.; Legzdins, P.; Martin, D. T. *Inorg. Chem.* **1978**, *17*, 3644. (f) Hunt, M. H.; Kita, W. G.; Mann, B. E.; McCleverty, J. A. *J. Chem. Soc., Dalton Trans.* **1978**, 467.

Table 7. Numbering Scheme, Yield, and Analytical Data for Complexes 1−13

| complex	complex no.	color (isolated yield, %)	anal. found (calcd)		
			C	H	N
$Cr(NO)(N^iPr_2)(O_2CPh)_2$	1	orange (75)	56.58 (56.60)	5.52 (5.70)	6.78 (6.60)
$CpCr(NO)(N^iPr_2)(O_2CPh)$	2	dark green (43)	58.83 (58.70)	6.50 (6.52)	7.56 (7.61)
$CpCr(NO)(N^iPr_2)(\eta^1\text{-}Cp)$	3	dark red (47)	61.61 (61.54)	7.55 (7.69)	8.80 (8.97)
$CpCr(NO)(N^iPr_2)(CH_2SiMe_3)$	4	red (69)	53.91 (53.89)	8.97 (8.98)	8.32 (8.38)
$CpCr(NO)(N^iPr_2)(\eta^1\text{-}CH_2Ph)$	5	red (45)	63.63 (63.91)	7.87 (7.69)	8.39 (8.28)
$CpCr(NO)(N^iPr_2)(Ph)$	6	red (42)	63.13 (62.96)	7.26 (7.41)	8.52 (8.64)
$CpCr(NO)(N^iPr_2)(CPh=CH_2)$	7	red (38)	65.05 (65.14)	7.44 (7.43)	7.57 (8.00)
$CpCr(NO)(N^iPr_2)(C\equiv CCMe_3)$	8	dark red-green (31)	62.42 (62.20)	8.72 (8.54)	8.38 (8.54)
$CpCr(NO)(N^iPr_2)(C\equiv CPh)$	9	dark red-green (54)	65.69 (65.52)	6.85 (6.90)	7.94 (8.05)
$Cr(NO)(N^iPr_2)(CH_2SiMe_3)_2$	10	dark red (85)	46.77 (47.15)	9.84 (10.17)	7.66 (7.86)
$Cr(NO)(N^iPr_2)(CH_2Ph)_2$	11	red-orange (47)	65.46 (65.91)[a]	7.41 (7.74)	7.45 (7.69)
$Cr(NO)(N^iPr_2)(o\text{-tolyl})_2$	12	dark red (39)	65.13 (65.91)[a]	7.72 (7.74)	7.47 (7.69)
$Cr(NO)(N^iPr_2)(CH_2SiMe_3)(C(=N^iBu)CH_2SiMe_3)$	13	dark red (53)	51.25 (51.94)[a]	10.18 (10.25)	9.26 (9.57)

[a] The carbon determination was repeatedly low despite numerous attempts with a variety of oxidizing agents.

Table 8. Mass Spectroscopic and IR Spectral Data for Complexes 1−13

complex no.	MS[a] (m/z)	probe temp (°C)	IR (Nujol, cm⁻¹)
1	394 ($P^+ - NO$)	150	1710 (s, ν_{NO}), 1599 (w), 1518 (w), 1493 (w), 1420 (w)
2	368 (P^+)	120	1668 (s, ν_{NO}), 1629 (m), 1574 (w), 1334 (m)
3	312 (P^+)	150	1670 (s, ν_{NO})
4	334 (P^+)	150	1660 (s, ν_{NO})
5	338 (P^+)	150	1661 (w, ν_{NO})
6	324 (P^+)	150	1644 (s, ν_{NO})
7	350 (P^+)	120	1676 (s, ν_{NO})
8	328 (P^+)	150	1667 (s, ν_{NO})
9	348 (P^+)	120	1670 (m, ν_{NO})
10	356 (P^+)	150	1670 (s, ν_{NO})
11	364 (P^+)	150	1634 (s, ν_{NO})
12	364 (P^+)	150	1620 (s, ν_{NO})
13	439 (P^+)	150	1609 (s, ν_{NO})

[a] Values for the highest intensity peak of the calculated isotopic cluster (^{52}Cr).

Cp anion produces $CpCr(NO)(N^iPr_2)(\eta^1\text{-}Cp)$ (**3**) (eq 4).

$$\text{(4)}$$
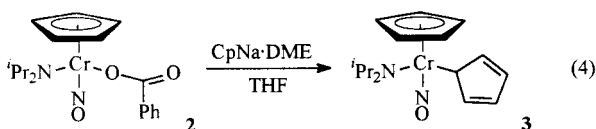
The 18e bis(cyclopentadienyl) complex **3** can also be generated directly from bis(benzoate) **1** by treatment with 2 equiv of Cp anion. Complex **3** contains one η^5- and one η^1-Cp ligand, as is clearly evident in its solid-state molecular structure (Figure 2 and Table 3). Similar structural features have been observed previously for $CpCr(NO)_2(\eta^1\text{-}Cp)$, $Cp_2Mo(NO)(\eta^1\text{-}Cp)$, and $CpMo(NO)(S_2CNR_2)(\eta^1\text{-}Cp)$.[29]

Other 18e hydrocarbyl complexes analogous to complex **3** can be conveniently prepared by the hydrocarbylation reactions of the Cp−benzoate complex **2** summarized in eq 5. The electronically saturated CpCr(NO)-

$$\text{(5)}$$
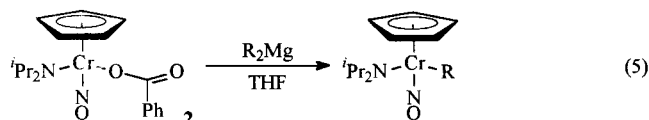
$(N^iPr_2)R$ complexes ($R = CH_2SiMe_3$ (**4**), η^1-CH_2Ph (**5**), Ph (**6**), CPh=CH₂ (**7**), C≡CCMe₃ (**8**), C≡CPh (**9**)) are the first well-characterized examples of Cr(II) nitrosyl

compounds containing σ-bonded hydrocarbyl ligands.[30] The hydrocarbyl ligands span a broad range of sizes, from the large CH_2SiMe_3 ligand to the less sterically demanding phenyl and alkynyl derivatives. The different electronic properties of these ligands are reflected in the varying values of $\nu(NO)$ for compounds **2**−**9** collected in Table 8. These bands suggest that the relative electron-donating power of the ligands to the $CpCr(NO)(N^iPr_2)$ fragment follows the order alkenyl < η^1-Cp ≈ benzoate ≈ alkynyl < benzyl ≈ CH_2SiMe_3 < phenyl. The ¹H NMR spectra for these compounds (Table 9) reveal that in each case all four amide Me groups are inequivalent, again implying that any rotation about the Cr−N bonds is slow on the NMR time scale at room temperature. That the specific orientation of this "locked" conformation is the planar ON−Cr−NC₂ alignment dictated by the respective π-bonding requirements of the nitrosyl and amide ligands is confirmed by the solid-state molecular structure of **4** (Figure 3).

Attempts to prepare other $CpCr(NO)(N^iPr_2)R$ compounds via the methodology shown in eq 5 were unsuccessful for R = Me or CH₂CMe₃. A possible reason for this failure is suggested by the byproducts of the thermolytic decomposition of complex **4**. When CpCr-(NO)(N^{i}Pr₂)(CH₂SiMe₃) is heated in C₆D₆ at 50 °C, the characteristic ¹H NMR spectroscopic features of **4** are diminished and resonances attributable to Me₄Si and Me₂C=N^{i}Pr are observable. These observations indicate that β-H abstraction from the amide methine group by the alkyl ligand may well be an important decomposition pathway for $CpCr(NO)(N^iPr_2)R$ species, as has been previously suggested for $Cr(N^iPr_2)$ alkyl nitride complexes.[25]

Electronically Unsaturated Hydrocarbyl Complexes. Coordinatively and electronically unsaturated chromium hydrocarbyl compounds of intermediate oxidation state (II−IV) are of interest as potential model complexes for heterogeneous, Cr-based olefin polymerization catalysts.[31] These mid-valent, open-shell organochromium species typically possess unpaired electrons, a property that reduces the utility of NMR

(30) $Cr(NO)(CH(SiMe_3)_2)_3$ has previously been proposed as the product of the reaction of $Cr(CH(SiMe_3)_2)_3$ with NO gas. However, this species was reported to be too unstable to be isolated and was characterized solely by solution IR spectroscopy: (a) Barker, G. K.; Lappert, M. F. *J. Organomet. Chem.* **1974**, *76*, C45. (b) Barker, G. K.; Lappert, M. F.; Howard, J. A. K. *J. Chem. Soc., Dalton Trans.* **1978**, 734.

(31) (a) Theopold, K. H. *CHEMTECH* **1997**, *27*(10), 26. (b) Theopold, K. H. *Eur. J. Inorg. Chem.* **1998**, *1*, 15.

Table 9. ^{1}H and ^{13}C{^{1}H} NMR Spectroscopic Data for Complexes 1−13

complex no.	^{1}H NMR^a δ (ppm)	^{13}C{^{1}H} NMR^a δ (ppm)	complex no.	^{1}H NMR^a δ (ppm)	^{13}C{^{1}H} NMR^a δ (ppm)
1^b	1.30 (br s, 6H, CH$_3$)	21.9 (CH$_3$)	**2**	0.62 (d, 3H, CH$_3$, J = 7 Hz)	20.3 (CH$_3$)
	1.88 (br s, 6H, CH$_3$)	28.5 (CH$_3$)		0.98 (d, 3H, CH$_3$, J = 7 Hz)	22.2 (CH$_3$)
	5.08 (br s, 1H, CH)	69.0 (CH)		1.30 (d, 3H, CH$_3$, J = 7 Hz)	26.7 (CH$_3$)
	6.62 (br s, 1H, CH)	70.6 (CH)		1.69 (d, 3H, CH$_3$, J = 7 Hz)	29.5 (CH$_3$)
	7.43 (vt, 4H, H$_m$, J_{app} = 7.8 Hz)	129.1 (CH$_o$/CH$_m$)		3.97 (m, 1H, CH)	65.0 (CH)
	7.57 (vt, 2H, H$_p$, J_{app} = 7.5 Hz)	130.0 (CH$_o$/CH$_m$)		5.40 (s, 5H, C$_5$H$_5$)	75.7 (CH)
	8.03 (d, 4H, H$_o$, J = 7.2 Hz)	131.5 (CCO$_2$)		5.51 (m, 1H, CH)	105.2 (C$_5$H$_5$)
		134.1 (CH$_p$)		7.15 (m, 3H, C$_6$H$_5$)	128.1 (CH$_o$/CH$_m$)
		182.5 (CO$_2$)		8.40 (m, 2H, C$_6$H$_5$)	130.3 (CH$_o$/CH$_m$)
					130.7 (CH$_p$)
					136.7 (CCO$_2$)
					171.2 (CO$_2$)
3	0.60 (d, 3H, CH$_3$, J = 6.2 Hz)	19.9 (CH$_3$)	**4**	0.37 (s, 9H, Si(CH$_3$)$_3$)	3.0 (Si(CH$_3$))
	0.78 (d, 3H, CH$_3$, J = 6.5 Hz)	20.5 (CH$_3$)		0.60 (d, 1H, CHH′, J = 11 Hz)	15.0 (CH$_2$)
	1.22 (d, 3H, CH$_3$, J = 6.5 Hz)	25.4 (CH$_3$)		0.65 (vt, 6H, CH$_3$, J_{app} = 7 Hz)	17.6 (CH$_3$)
	1.70 (d, 3H, CH$_3$, J = 6.5 Hz)	30.7 (CH$_3$)		0.82 (d, 1H, CH$H′$, J = 11 Hz)	20.3 (CH$_3$)
	3.70 (m, 1H, CH)	62.0 (CH)		1.38 (d, 3H, CH$_3$, J = 7 Hz)	25.8 (CH$_3$)
	4.40 (m, 1H, CH)	72.2 (CH)		1.62 (d, 3H, CH$_3$, J = 7 Hz)	30.0 (CH$_3$)
	4.59 (s, 5H, η^5-C$_5$H$_5$)	105.0 (η^5-C$_5$H$_5$)		3.65 (m, 1H, CH)	60.8 (CH)
	6.39 (s, 5H, η^1-C$_5$H$_5$)	116.2 (br, η^1-C$_5$H$_5$)		4.25 (m, 1H, CH)	71.0 (CH)
				5.17 (s, 5H, C$_5$H$_5$)	102.2 (C$_5$H$_5$)
5	0.63 (d, 3H, CH$_3$, J = 7 Hz)	18.3 (CH$_3$)^c	**6**^{d}	0.91 (d, 3H, CH$_3$, J = 7 Hz)	18.9 (CH$_3$)
	0.70 (d, 3H, CH$_3$, J = 7 Hz)	20.6 (CH$_3$)		1.23 (vt, 6H, CH$_3$, J_{app} = 7 Hz)	21.5 (CH$_3$)
	1.40 (d, 3H, CH$_3$, J = 7 Hz)	25.3 (CH$_3$)		1.45 (d, 3H, CH$_3$, J = 7 Hz)	26.1 (CH$_3$)
	1.70 (d, 3H, CH$_3$, J = 7 Hz)	30.9 (CH$_3$)		4.10 (m, 1H, CH)	30.8 (CH$_3$)
	2.68 (d, 1H, CHH′, J = 11 Hz)	37.6 (CH$_2$)		5.07 (m, 1H, CH)	62.2 (CH)
	3.70 (m, 1H, CH)	61.0 (CH)		5.56 (s, 5H, C$_5$H$_5$)	73.0 (CH)
	3.70 (d, 1H, CH$H′$, J = 11 Hz)	71.3 (CH)		6.92 (t, 1H, CH$_p$, J = 5 Hz)	103.8 (C$_5$H$_5$)
	4.30 (m, 1H, CH)	103.1 (C$_5$H$_5$)		7.01 (vt, 2H, CH$_m$, J_{app} = 5 Hz)	124.5 (CH$_p$)
	4.95 (s, 5H, C$_5$H$_5$)	123.0 (CH$_p$)		7.51 (d, 2H, CH$_o$, J = 5 Hz)	127.4 (CH$_o$/CH$_m$)
	6.98 (m, 1H, H$_p$)	153.3 (C$_{ipso}$)			138.7 (CH$_o$/CH$_m$)
	7.22 (m, 2H, H$_o$/H$_m$)				171.0 (C$_{ipso}$)
	7.50 (m, 2H, H$_o$/H$_m$)				
7^e	0.41 (d, 3H, CH$_3$, J = 6.4 Hz)	18.5 (CH$_3$)^f	**8**^{g}	0.61 (d, 3H, CH$_3$, J = 7 Hz)	18.9 (CH$_3$)
	0.67 (d, 3H, CH$_3$, J = 6.5 Hz)	12.0 (CH$_3$)		1.18 (d, 3H, CH$_3$, J = 7 Hz)	19.6 (CH$_3$)
	1.36 (d, 3H, CH$_3$, J = 6.5 Hz)	26.5 (CH$_3$)		1.30 (d, 3H, CH$_3$, J = 7 Hz)	26.0 (CH$_3$)
	1.55 (d, 3H, CH$_3$, J = 6.5 Hz)	61.9 (CH)		1.40 (s, 9H, C(CH$_3$)$_3$)	29.8 (CH$_3$)
	3.65 (m, 1H, CH)	73.0 (CH)		1.95 (d, 3H, CH$_3$, J = 7 Hz)	32.4 (C(CH$_3$)$_3$)
	4.31 (m, 1H, CH)	103.2 (C$_5$H$_5$)		3.90 (m, 1H, CH)	62.7 (C(CH$_3$)$_3$)
	5.21 (s, 5H, C$_5$H$_5$)	120.2 (C=CH$_2$)		4.50 (m, 1H, CH)	62.9 (CH)
	5.36 (d, 1H, CHH′, J = 1.7 Hz)	125.0 (CH$_p$)		5.25 (s, 5H, C$_5$H$_5$)	73.1 (CH)
	6.08 (d, 1H, CH$H′$, J = 1.7 Hz)	127.1 (CH$_o$/CH$_m$)			102.5 (C$_5$H$_5$)
	7.04 (m, 1H, CH$_p$)	128.2 (CH$_o$/CH$_m$)			106.7 (C≡CC(CH$_3$)$_3$)
	7.20 (m, 2H, CH$_o$/CH$_m$)	155.9 (C$_{ipso}$)			133.1 (C≡CC(CH$_3$)$_3$)
	7.22 (m, 2H, CH$_o$/CH$_m$)	180.7 (C=CH$_2$)			
9^g	0.58 (d, 3H, CH$_3$, J = 7 Hz)	19.9 (CH$_3$)^h	**10**	0.20 (d, 2H, CHH′, J = 6.6 Hz)	2.54 (Si(CH$_3$)$_3$)
	1.10 (d, 3H, CH$_3$, J = 7 Hz)	20.4 (CH$_3$)		0.32 (s, 18H, Si(CH$_3$)$_3$)	21.3 (br, CH$_3$)
	1.38 (d, 3H, CH$_3$, J = 7 Hz)	27.2 (CH$_3$)		0.92 (br s, 6H, CH$_3$)	28.1 (br, CH$_3$)
	1.90 (d, 3H, CH$_3$, J = 7 Hz)	30.2 (CH$_3$)		1.14 (br s, 6H, CH$_3$)	68.1 (CH$_2$)
	3.90 (m, 1H, CH)	63.7 (CH)		1.99 (d, 2H, CH$H′$, J = 6.6 Hz)	49.0 (br, CH)
	4.50 (m, 1H, CH)	74.3 (CH)		3.28 (v br s, 1H, CH)	55.9 (br, CH)
	5.22 (s, 5H, C$_5$H$_5$)	102.8 (C$_5$H$_5$)		4.36 (v br s, 1H, CH)	
	7.01 (m, 1H, CH$_p$)	125.5 (CH$_p$)			
	7.10 (m, 2H, CH$_o$/CH$_m$)	127.9 (CH$_o$/CH$_m$)			
	7.60 (m, 2H, CH$_o$/CH$_m$)	130.5 (CH$_o$/CH$_m$)			
11	0.72 (br s, 6H, CH$_3$)	20.6 (br, CH$_3$)	**12**	1.04 (d, 3H, CH$_3$, J = 6.0 Hz)	18.9 (CH$_3$)^i
	1.19 (br s, 6H, CH$_3$)	27.3 (br, CH$_3$)		1.19 (d, 3H, CH$_3$, J = 6.1 Hz)	24.2 (CH$_3$)
	1.72 (d, 2H, CHH′, J = 7.0 Hz)	42.8 (br, CH)		1.29 (d, 6H, CH$_3$, J = 5.8 Hz)	25.1 (CH$_3$)
	2.20 (v br s, 1H, CH)	53.6 (CH$_2$)		2.40 (s, 3H, PhCH_3)	25.4 (CH$_3$)
	2.85 (d, 2H, CH$H′$, J = 7.0 Hz)	56.4 (br, CH)		2.77 (s, 3H, PhCH_3)	25.7 (CH$_3$)
	3.22 (v br s, 1H, CH)	125.8 (CH$_p$)		4.49 (m, 1H, CH)	27.7 (CH$_3$)
	6.81 (m, 4H, C$_6$H$_5$)	129.1 (CH$_o$/CH$_m$)		4.68 (m, 1H, CH)	61.7 (CH)
	7.00 (m, 6H, C$_6$H$_5$)	130.5 (CH$_o$/CH$_m$)		6.73−7.17 (m, 6H, H$_m$/H$_p$)	64.5 (CH)
		138.1 (C$_{ipso}$)		8.00 (d, 1H, H$_o$, J = 7.6 Hz)	124.5 (C$_{aromatic}$)
				8.13 (d, 1H, H$_o$, J = 6.9 Hz)	126.0 (C$_{aromatic}$)
					127.0 (C$_{aromatic}$)
					127.7 (C$_{aromatic}$)
					129.0 (C$_{aromatic}$)
					2 × 130.0 (C$_{aromatic}$)
					141.3 (C$_{aromatic}$)
					143.0 (C$_{aromatic}$)
					161.6 (C$_{aromatic}$)
					177.4 (C$_{aromatic}$)
13^j	0.03 (s, 9H, Si(CH$_3$)$_3$)	0.3 (Si(CH$_3$)$_3$)	**13**^{j}	1.82 (d, 1H, CH$H′$, J = 9.9 Hz)	30.3 (C(CH$_3$)$_3$)
	0.22 (s, 9H, Si(CH$_3$)$_3$)	3.0 (Si(CH$_3$)$_3$)		2.93 (d, 1H, −CCHH′Si(Me)$_3$, J = 11.4 Hz)	31.1 (CH$_2$)
	0.68 (d, 1H, CHH′, J = 9.9 Hz)	19.2 (CH$_3$)		3.00 (m, 1H, CH)	53.2 (CH)
	0.70 (d, 3H, CH$_3$, J = 6.3 Hz)	22.2 (CH$_3$)		3.30 (d, 1H, CCH$H′$Si(Me$_3$), J = 11.1 Hz)	56.2 (CH)
	0.91 (d, 3H, CH$_3$, J = 6.3 Hz)	23.7 (CH$_2$)		3.56 (m, 1H, CH)	62.1 (C(CH$_3$)$_3$)
	1.50 (s, 9H, C(CH$_3$)$_3$)	28.3 (CH$_3$)			220.8 (C=N)
	1.56 (vt, 6H, CH$_3$, J_{app} = 6.0 Hz)	29.5 (CH$_3$)			

^{a} ^{1}H and ^{13}C{^{1}H} NMR spectra recorded in C$_6$D$_6$ at room temperature unless otherwise noted. ^{b} Spectra recorded in THF-d_8. ^{c} The CH$_o$ and CH$_m$ signals were obstructed by the solvent signal. ^{d} Spectra recorded in CD$_3$CN. ^{e} ^{13}C{^{1}H} spectrum recorded in (CD$_3$)$_2$CO. ^{f} The fourth methyl signal was obstructed by the solvent signal. ^{g} ^{13}C{^{1}H} spectrum recorded in CDCl$_3$. ^{h} The C$_{ipso}$ and two quaternary acetylide carbon signals were not observed in the spectrum. ^{i} One aromatic signal was obstructed by the solvent signal. ^{j} Spectra recorded in CDCl$_3$.
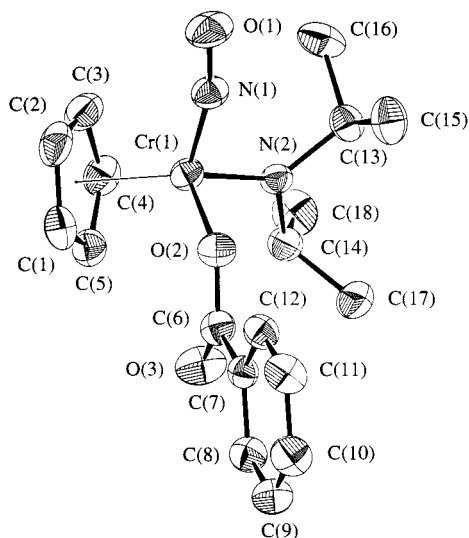
Figure 1. Solid-state molecular structure of complex **2** (33% probability thermal ellipsoids are shown).
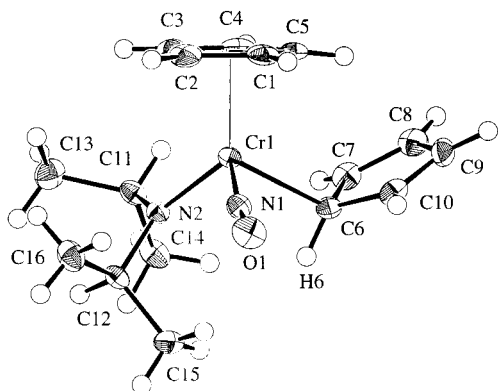

Figure 2. Solid-state molecular structure of complex **3** (50% probability thermal ellipsoids are shown).
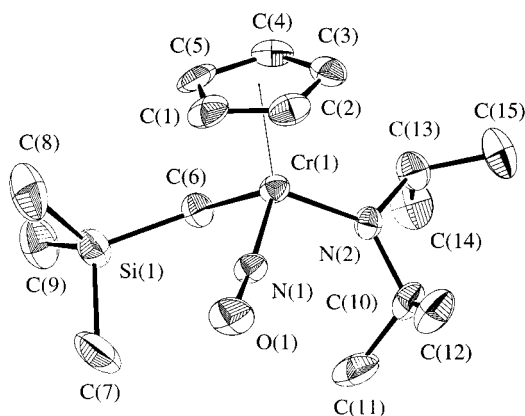

Figure 3. Solid-state molecular structure of complex **4** (50% probability thermal ellipsoids are shown).

spectroscopy, the primary reaction-monitoring technique employed in homogeneous organometallic chemistry. However, it is not unreasonable to expect that if the spin-pairing and orbital-splitting energies of such compounds were properly manipulated by their ancillary ligands, *diamagnetic* unsaturated chromium alkyl complexes might then be attainable.

Such species could in principle be generated from the $CpCr(NO)(N^iPr_2)R$ compounds described in the preceding section if the amide group could be replaced with a
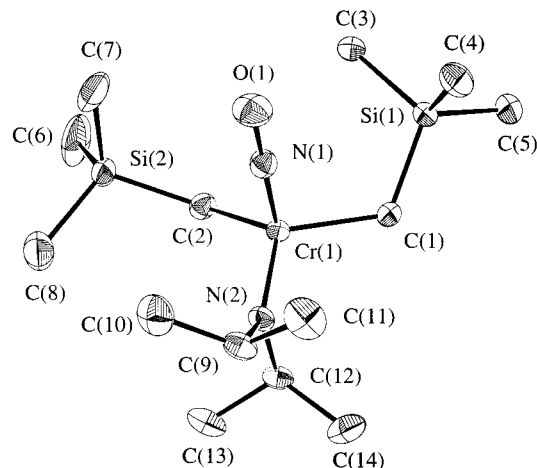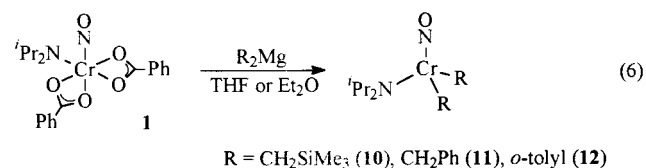

Figure 4. Solid-state molecular structure of complex **10** (50% probability thermal ellipsoids are shown).

halide or hydrocarbyl ligand. Although theoretical studies suggest that compounds such as $CpCr(NO)(R)Cl$ and $CpCr(NO)(NR_2)Cl$ should be less prone to loss of nitric oxide than is $CpCr(NO)Cl_2$,[4] such complexes have yet to be isolated or even spectroscopically detected in any of the reactions that we have attempted to date. Comparatively mild reagents fail to react with the amide alkyl species, and more harsh reagents such as anhydrous HCl in Et_2O lead to decomposition to non-nitrosyl-containing Cr(III) species.[6]

Fortunately, unsaturated hydrocarbyl compounds *are* obtainable by the direct hydrocarbylation of bis(benzoate) complex **1** with organomagnesium reagents (eq 6). The novel $Cr(NO)(N^iPr_2)R_2$ products (R = CH$_2$SiMe$_3$

$$^{i}Pr_2N-Cr\begin{matrix} O \\ \| \\ N \end{matrix} \underset{O}{\overset{O}{\diagdown}} Ph \xrightarrow[\text{THF or Et}_2O]{R_2Mg} {}^{i}Pr_2N-Cr\overset{\overset{O}{\|}}{\underset{R}{\diagdown}}R \qquad (6)$$

$$\text{Ph} \qquad \mathbf{1}$$

R = CH$_2$SiMe$_3$ (**10**), CH$_2$Ph (**11**), *o*-tolyl (**12**)

(**10**), CH$_2$Ph (**11**), *o*-tolyl (**12**)) are isolable as red, diamagnetic solids that are sensitive to both air and moisture. The solid-state molecular structures of **10** (Figure 4 and Table 5) and **11** (Figure 5 and Table 6) have been established by single-crystal X-ray crystallography, and they exhibit some interesting features. For instance, the metrical parameters of both structures provide evidence for the presence of strong Cr–N(amide) π-bonding interactions. Indicative of the strong π-bonds present in all of the molecular structures reported in this paper are the N(nitrosyl)–Cr–N(amide)–C torsion angles, which fall within 4° of 0 and 180°.[6] The Cr–NO bonds in **10** and **11** remain in the planes defined by the Cr–NC$_2$ units, and the Cr–N amide bond lengths of 1.763(2) Å in **10** and 1.772(2) Å in **11** are even shorter than those extant in complexes **2**–**4**.[27] Furthermore, one benzyl ligand in **11** is attached in a η^1 fashion to the metal center and functions as a one-electron donor, whereas the other is attached in an η^2 mode and provides three electrons to the central chromium.[32]

(32) For related bis(benzyl) complexes of molybdenum and tungsten, see: (a) Legzdins, P.; Jones, R. H.; Phillips, E. C.; Yee, V. C.; Trotter, J.; Einstein, F. W. B. *Organometallics* **1991**, *10*, 986. (b) Dryden, N. H.; Legzdins, P.; Trotter, J.; Yee, V. C. *Organometallics* **1991**, *10*, 2857 and references therein. (c) Reference 27b.
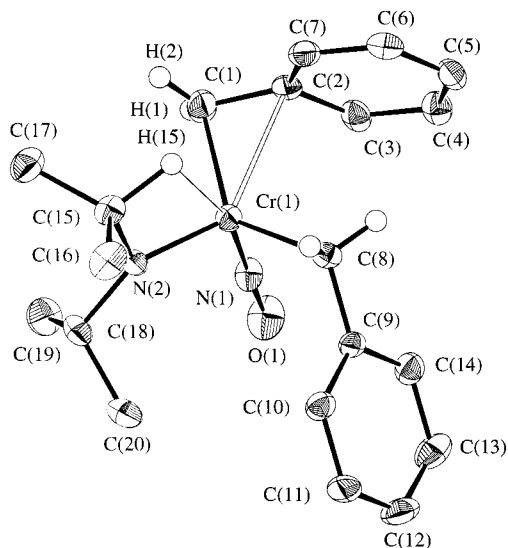
Figure 5. Solid-state molecular structure of complex **11** (50% probability thermal ellipsoids are shown).

There is also an agostic interaction involving the chromium and the C(15)−H(15) bond, as indicated by the refined Cr(1)−H(15) distance of 2.12(2) Å and the Cr(1)−N(2)−C(15) angle of 105.32(15)°, which is much smaller than the expected 120°. Consistently, the Cr(1)−N(2)−C(18) angle has expanded to 137.36(15)°. The solid-state structure of **10** also exhibits metrical parameters indicative of a similar agostic interaction, even though the relevant hydrogen atom was not located and refined in this case. Nevertheless, the distortions of the angles at N(2) (i.e. Cr(1)−N(2)−C(12) = 103.2-(2)° and Cr(1)−N(2)−C(9) = 138.4(2)°) are even more pronounced than in **11**. Overall **10** has a flattened, pseudotetrahedral geometry about the chromium center.

The spectroscopic properties of **10** and **11** (presented in Tables 8 and 9) indicate that these complexes are stereochemically nonrigid in solution. The room-temperature ¹H NMR spectrum of **10** in toluene-d_8 exhibits two broad singlets corresponding to the amide ligand methyl groups. This is an indication that a single fluxional process is occurring in this compound, namely rotation about the Cr−amide bond. When the NMR sample is warmed, these two signals move closer together and coalesce at 32 °C with a chemical shift of 1.06 ppm. Further warming to 60 °C results in equilibration of the four methyl groups and thus one sharp signal in the spectrum exhibiting 7 Hz coupling to the methine protons. Cooling of the sample to −60 °C produces a limiting spectrum with the two signals further separated and methine proton coupling only slightly visible. Using this variable-temperature NMR data, it is possible to calculate $\Delta G^{\ddagger}_{305\ K}$, the barrier to this fluxional process, to be 14.1(1) kcal mol⁻¹, which falls in the expected range for this type of process.[25b,33]

It is also possible to study the methine protons and obtain a measure of the barrier to rotation using their ¹H NMR signals. In this case, two very broad singlets are present in the room-temperature spectrum, which shift toward each other upon warming and coalesce at 49 °C with a chemical shift of 3.85 ppm. The signals

separate and sharpen moderately upon cooling of the sample to −60 °C, although coupling to the methyl protons is not visible. Calculation of $\Delta G^{\ddagger}_{322\ K}$ using these resonances gives the nearly identical result of 14.2(1) kcal mol⁻¹.

Another interesting feature is the significant variance of the spectra with solvent. For example, in CD_2Cl_2 the methyl signals have already gone past coalescence at room temperature, suggesting that in polar solvents rotation of the amide ligand is faster. This observation can be rationalized by considering that a polar solvent is able to draw electron density from the Cr−amide bond, thus weakening the interaction and facilitating the fluxional process.

Similarly, a variable-temperature ¹H NMR study was undertaken for compound **11**. This showed that the amide fluxional processes occurring in this compound are analogous to those in **10**. However, in addition to amide ligand rotation, there is also the added element of observing the two benzyl ligand interactions. In contrast to the solid-state molecular structure of **11**, the η^2-benzyl interaction is not detected in solution either at room temperature or at −63 °C. Clearly in solution the two benzyl ligands are "switching" from η^1 to η^2 at a rate more rapid than the NMR time scale. At low temperature slight broadening of the aromatic signals occurs, thereby suggesting that these signals are beginning to decoalesce.[32]

The agostic interaction is also absent in solution, as evidenced by gated ¹³C{¹H} NMR spectroscopy. At −63 °C the coupling constant for one of the methine carbon signals is 144 Hz while the other is reduced to 118 Hz. The latter value is not small enough to indicate an agostic interaction conclusively, but it does demonstrate that the two methine environments are indeed different. Much sharper amide resonances and distinct aromatic signals appear in the ¹H NMR spectrum of the aryl derivative **12**, presumably due to the increased steric demands of the ortho-substituted ligand. The net effect is a slowing of the rotation of the amide moiety and an inequivalent orientation of the o-tolyl ligands.

As would be expected for coordinatively and electronically unsaturated compounds, **10**−**12** exhibit reactivity toward a variety of small molecules. For example, preliminary investigations indicate that t-BuNC can be inserted into the bis(alkyl) complex **10** to generate **13**, as shown in eq 7.[25b] Further reactivity studies are currently in progress.
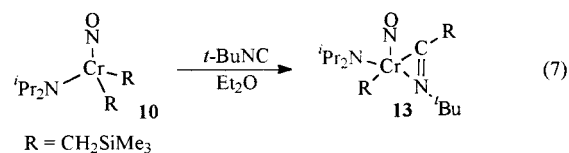
Epilogue

Understanding precisely why Cr(NO)(N^{i}Pr$_2$)R$_2$ complexes are diamagnetic is an issue with potentially important ramifications. While great advances have recently been made in olefin polymerization catalyzed by homogeneous, organometallic compounds of Ti and Zr,[34] the paramagnetic nature of unsaturated Cr alkyl species has reduced their effectiveness as model compounds for providing analogous insights into the de-

(33) Chisholm, M. H.; Folting, K.; Huffman, J. C.; Rothwell, I. P. *Organometallics* **1982**, *1*, 251.

tailed mechanism of commercially applicable, heterogeneous, Cr-based polymerization systems.[31] Similar obstacles will undoubtedly beset investigation of Fe and Co model compounds in the wake of the recent development of paramagnetic polymerization catalysts based on these later first-row metals.[35] Diamagnetic, midvalent, unsaturated alkyl compounds of these metals are desirable both for practical reasons (increased utility of NMR techniques) and for more fundamental concerns (potential comparisons to gauge the role of spin state).[36] The characteristic reactivities of $Cr(NO)(N^iPr_2)R_2$ compounds, as well as an evaluation of the factors which contribute to their spin-paired electronic configuration, will be the subjects of a later publication.[37]

Conclusions

$Cr(NO)(N^iPr_2)_3$ has proven to be a useful synthetic precursor to diamagnetic Cr(II) nitrosyl compounds containing σ-hydrocarbyl ligands. Selective amine elimination of two N^iPr_2 groups occurs upon treatment with benzoic acid, and the resulting O_2CPh ligands are readily exchanged via salt metatheses. The $CpCr(NO)(N^iPr_2)$ fragment readily supports a wide variety of R ligands, although some of the alkyl derivatives are thermally sensitive. Routes to $Cp'Cr(NO)R_2$ compounds remain to be devised, since this class of Cr(II) alkyl compounds is not accessible from $CpCr(NO)(N^iPr_2)X$ precursors. However, unsaturated organochromium(II) compounds with an even greater degree of unsaturation can be obtained via the dialkylation of $Cr(NO)(N^iPr_2)(O_2CPh)_2$.

Supporting Information Available: Full details of the crystallographic analyses, including tables of crystallographic data, atomic coordinates, bond lengths, bond angles, hydrogen atom coordinates, anisotropic displacement parameters, torsion angles, and selected nonbonded contacts for complexes **2**−**4**, **10**, and **11**. This material is available free of charge via the Internet at http://pubs.acs.org.

OM980954M

(34) (a) Brintzinger, H. H.; Fischer, D.; Mülhaupt, R.; Rieger, B.; Waymouth, R. M. *Angew. Chem., Int. Ed. Engl.* **1995**, *34*, 1143. (b) Obora, Y.; Stern, C. L.; Marks, T. J.; Nickias, P. N. *Organometallics* **1997**, *16*, 2503. (c) Halterman, R. L.; Tretyakov, A.; Kahn, M. A. *J. Organomet. Chem.* **1998**, *568*, 41. (d) Bravakis, A. M.; Bailey, C. E.; Pigeon, M.; Collins, S. *Macromolecules* **1998**, *31*, 1000.

(35) (a) Britovsek, G. J. P.; Gibson, V. C.; Kimberley, B. S.; Maddox, P. J.; McTavish, S. J.; Solan, G. A.; White, A. J. P.; Williams, D. J. *Chem. Commun.* **1998**, 849. (b) Small, B. L.; Brookhart, M.; Bennett, M. A. *J. Am. Chem. Soc.* **1998**, *120*, 4049. (c) Small, B. L.; Brookhart, M. *J. Am. Chem. Soc.* **1998**, *120*, 7143.

(36) Poli, R. *Chem. Rev.* **1996**, *96*, 2135.

(37) Jandciu, E. W.; Legzdins, P. Work in progress.